ACS Partner Journal
PRECISION CHEMISTRY
Editors' Choice
Open Access

pubs.acs.org/PrecisionChem
Letter

Stepwise Chemical Reduction of [4]Cyclo[4]helicenylene: Stereo Transformation and Site-Selective Metal Complexation

Zheng Zhou,* Yong Yang,* Jianwei Liang, Sota Sato, Zhenyi Zhang, and Zheng Wei

Cite This: *Precis. Chem.* 2025, 3, 27−34
Read Online

ACCESS | Metrics & More | Article Recommendations | Supporting Information

ABSTRACT: A highly strained macrocycle comprising four [4]helicene panels, [4]cyclo[4]helicenylene ([4]CH, **1**), was synthesized through a one-pot macrocyclization and chemically reduced by alkali metals (Na and K), revealing a four-electron reduction process. The resulting di-, tri-, and tetraanions of compound **1** were isolated and crystallographically characterized by X-ray diffraction. Owing to the four axially chiral bi[4]helicenyl fragments, a reversible stereo transformation of **1** between the (*S*,*R*,*S*,*R*)- and (*S*,*S*,*R*,*R*)-configurations was disclosed upon the two-electron uptake, which was rationally understood by theoretical calculations. The (*S*,*S*,*R*,*R*)-configuration of $\mathbf{1}^{2-}$ was further stabilized in triply reduced and tetra-reduced states, where structural deformation led by charges and metal complexation was observed. This study proposed an approach to alter the configuration of cycloarylenes in addition to thermal treatment.

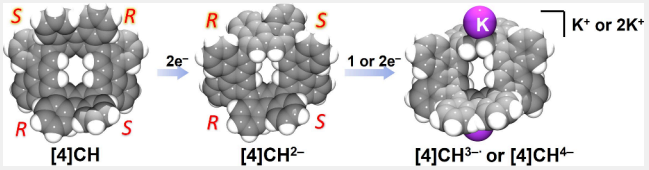

KEYWORDS: *cycloarylene, chemical reduction, stereo transformation, axial chirality, X-ray diffraction, metal complexation*

The chemistry of hydrocarbon cycloarylenes is an interesting subject for chemists owing to the aesthetic beauty of three-dimensional topologies,[1−4] the unique physical and electronic properties,[5,6] that they are ideal supramolecular hosts,[7−11] as well as that they are promising candidates in functional materials.[12−14] Since the pioneering work of the syntheses of *ortho*-,[15−17] *meta*-,[18,19] and *para*-linked phenylenes,[20] recent decades have witnessed the glorious synthetic advancement of cycloarylenes that paves the road to an in-depth exploration of their properties and applications.[14,21−23] The introduction of chirality in a cyclic π-system, such as *R*/*S* axial,[24−28] *M*/*P* helical,[29−34] and *E*/*Z* coplanar,[35−37] not only affords structurally appealing molecules but fascinates chemists with potential chiroptical properties such as CD and CPL.[38−42] Thus, the stereoisomerism in cycloarylenes arising from the rotation behavior of biaryl fragments or helicene units[43] deserves an elaborate consideration.

Cycloarylenes, particularly [*n*]cycloparaphenylenes ([*n*]-CPPs), exhibit intriguing redox chemistry and structural responses in terms of their unusual HOMO−LUMO gap trends,[44,45] allowing remarkable interest in organic electroconductive or energy storage materials.[46−49] It has been demonstrated that chemical reduction gives rise to structural deformation of polycyclic aromatic hydrocarbons (PAHs).[50−55] In particular, [*n*]CPPs underwent elliptical and quinoidal distortion upon two-electron uptake (Scheme 1a);[56−59] [6]cyclo-2,7-naphthylene ([6]CNAP) underwent a two-electron reduction with an emergence of π-extension over the binaphthyl linkages and global aromaticity.[60] Moreover, chemical reduction facilitated reversible core dimerization/transformation[61−64] and ring-closure/cleavage in some cases,[65−67] indicating its tremendous energy for selective

Scheme 1. Reduction-Induced Deformation or Stereo Transformation of Cycloarylenes

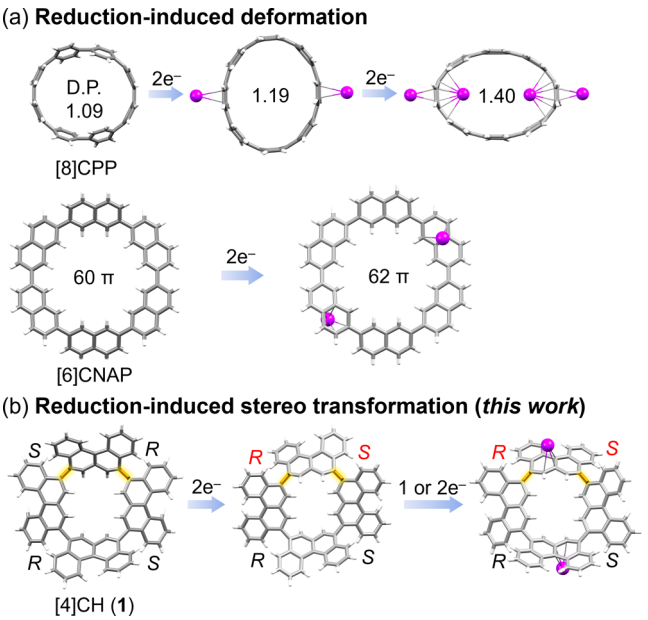

Received: August 2, 2024
Revised: October 16, 2024
Accepted: October 17, 2024
Published: November 1, 2024

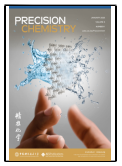

https://doi.org/10.1021/prechem.4c00064
Precis. Chem. 2025, 3, 27−34

bond activation. Although the thermally induced isomerization has been widely used to promote the interconversion of cycloarylene stereoisomers,[24−37] the transformation related to the *R*/*S*-, *M*/*P*-, or *E*/*Z*-configuration driven by a chemical reduction has never been disclosed or explored. Herein, we present the first chemical reduction-induced stereo transformation study, using [4]cyclo[4]helicenylene ([4]CH, Scheme 1b) as a platform. [4]CH is a hydrocarbon macrocycle bearing four constrained bi[4]helicenyl (BH) fragments with *R*/*S*-configuration, and it was synthesized by one-pot macrocyclization of a [4]helicene panel. [4]CH was able to be reduced by alkali metals (Na and K), and the generated doubly, triply, and quadruply reduced species were isolated and characterized by single-crystal X-ray diffraction. Compared to that of neutral [4]CH, their π-framework showed a different *R*/*S* configuration that was even not detected upon synthesis or by thermal isomerization. This intriguing reversible *R*/*S* stereo transformation and site-selective metal complexation were understood by theoretical investigation.

Ni-mediated Yamamoto-type coupling is widely employed as a synthetic tool to afford a diversity of cycloarylenes (Scheme S1).[68−71] To our surprise, by using one-pot macrocyclization of the monomer 5,8-dibromobenzo[*c*]phenanthrene, more strained [4]CH (**1**, strain energy: 33.6 kcal/mol, Table S9) and [5]CH (**2**, 12.5 kcal/mol) were isolated as the dominant products in yields of 7% and 9%, respectively (Figures S1−3). We surmised that the constrained BH fragments would be the rationale due to their rotation behaviors that provided an opportunity for the assembly of four 5,8-[4]helicene panels in a pseudo perpendicular fashion as found from the large dihedral angle of BH fragments in **1** (vide infra).

To determine the interesting stereochemistry of strained [4]CH (**1**), we first performed SC-XRD measurements to determine its crystal structure. By selection of proper crystallization conditions, **1** can present in different crystalline forms, suggesting the great adaptability of its π-framework. For instance, the evaporation of the tetrachloroethane solution of **1** afforded colorless plate-shaped crystals as a solvated structure $C_{72}H_{40}\cdot 1.7C_2H_2Cl_4$ (**1-t**, t stands for tetrachloroethane, Figure S19), while the slow cooling of the mixture of melted anthracene[72] and **1** resulted in the formation of a new polymorph containing one-half of an anthracene molecule, $C_{72}H_{40}\cdot 0.5C_{14}H_{10}$ (**1-a**, a stands for anthracene, Figure S20). To exclude the solvent effects, sublimation of **1** in vacuo at 285 °C was applied for the crystal growth that contributed to a new nonsolvated polymorph, **1-n** (n stands for nonsolvated, Figures 1a,b and S23). In the solid-state structure of **1-n**, **1** exhibited a dihedral angle of 82°, −66°, 66°, and −82° for BH1, BH2, BH3, and BH4, respectively, larger than those for biaryls in [4]CPhen$_{2,9}$ (avg 66°)[27] and [6]cyclo-1,3-pyrenylene (avg 64°).[71] Such remarkably large dihedral angles helped to relieve steric hindrance at fjord BH linkages and ring strain. The **1-n** molecules were stacked into a 1D column through C−H···π interactions (2.568(15)−2.733(15) Å) between the peripheral phenyl rings (Figure 1c), while no significant interactions were found between adjacent columns (Figure 1d). In contrast, the insertion of anthracene molecules expanded the width of the column to 22.5 Å from 17.0 Å in **1-a** (Figure 1e), which was observed in every other column with C−H···π contacts of 2.588(6)−2.641(6) Å (Figure 1f). In all three crystalline forms, **1** adopted an identical π-framework of the (*S*,*R*,*S*,*R*)-configuration, in agreement with the conformational search

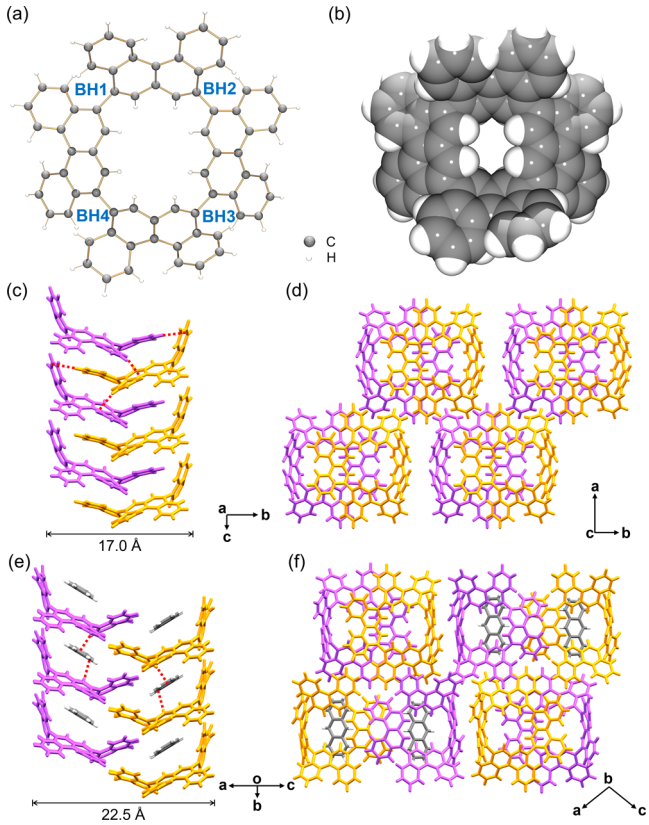

Figure 1. Crystal structure of **1-n** in (a) ball-and-stick and (b) space-filling models, 1D columns of (c) **1-n** and (e) **1-a**, and solid-state structures of (d) **1-n** and (f) **1-a** in capped-stick models.[1] The adjacent molecules are colored purple and orange for clarity, and C−H···π interactions are colored as red dotted lines.

calculations (Figure S39), which indicated that the obtained **1** upon synthesis is a *meso* isomer.

Compared to **1**, the addition of one more [4]helicene panel endows the *R*/*S* chirality of **2**. By using a cholesterol-loaded silica gel column under HPLC conditions, two enantiomers of **2** were separated (Figure S3) and showed mirror-imaged signals in the CD spectra (Figure S5). Slow evaporation of **2** and one of the enantiomers in different solvents afforded racemic (**2-r**) and enantiopure polymorphs (**2-e**), respectively (see the Supporting Information for details, Figures S21−22 and S27−28). Furthermore, the VT CD spectra showed that the racemization of **2-e** underwent a first-order reaction correlated with the equation $\ln([CD]_t/[CD]_0) = -kt$, and the rate constant of 2.2×10^{-4} s^{-1} was estimated at 80 °C. The temperature dependence of the rate constant was elucidated with the Eyring equation $k = \kappa(k_BT/h)\exp(-\Delta G^{\ddagger}/RT)$ to provide the energy barrier of $\Delta G^{\ddagger}$ = +28.2 kcal/mol at 298 K (Figures S6−9). In contrast, no other diastereomers of [4]CH were found according to HPLC analysis when heating a solution of **1** at over 200 °C for 1 week, possibly owing to their much higher energy level (Figure S38) that makes them thermodynamically unfavored.

Given the ineffectiveness of thermally induced isomerization of **1** to provide the other [4]CH diastereomers with different *R*/*S*-configurations, we turned our attention to exploring whether electron addition could trigger a conformational transformation of cylco[*n*]helicenylenes using **1** as a representative model. The chemical reduction of **1** was studied at room temperature in THF with sodium and potassium

https://doi.org/10.1021/prechem.4c00064
Precis. Chem. 2025, 3, 27−34

metals (Scheme 2), which was monitored by time-dependent UV−vis spectroscopy (Figures S14−15). As shown in Figure S16, the reaction proceeded with a pink color initially (monoanion), followed by a red-brown color (dianion) and violet color (trianion), and finally turned blue, which was associated with the last reduction stage (tetraanion). By slow diffusion of hexanes into the THF filtrate in the presence of 18-crown-6 ether, the products at different stages were isolated as high-quality single crystals (see the Supporting Information for details, Table S2). The SC-XRD experiments confirmed the formation of a solvent-separated ion product $[Na^+(18\text{-crown-}6)(THF)_2]_2[\mathbf{1}^{2-}]$ (**3**), a contact ion pair $[K^+(18\text{-crown-}6)(THF)_2][\{K^+(18\text{-crown-}6)(THF)\}_2(\mathbf{1}^{3-\bullet})]$ (**4**, crystallized with two interstitial THF molecules as **4**·2THF), and a contact ion product $[K^+(18\text{-crown-}6)(THF)_2]_2[\{K^+(18\text{-crown-}6)\}_2(\mathbf{1}^{4-})]$ (**5**). The bulk purity of **3**−**5** was confirmed by powder XRD (Figures S34−36 and Tables S6−8). It should be mentioned that the crystallization of monoanionic **1** was missed, presumably because of its instability. Chemical reduction of **2** was also performed (Figures S17−18); however, we failed to obtain the high-quality crystals of **2** in any charged states.

Scheme 2. Chemical Reduction of 1 and Preparation of Complexes 3−5

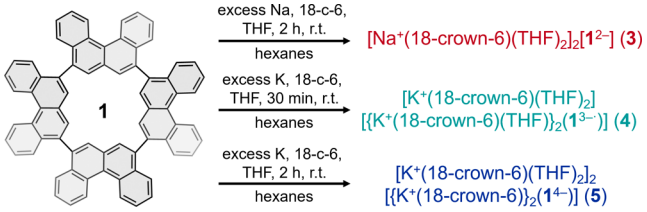

In the crystal structure of **3** (Figures 2a, S24, and S29), the $[Na^+(18\text{-crown-}6)(THF)_2]$ moieties were solvent-separated from the dianionic core $\mathbf{1}^{2-}$, allowing the evaluation of the core deformation upon electron addition without any metal binding influence. The Na^+ ion was entrapped by an 18-crown-6 ether molecule ($Na\cdots O_{crown}$: 2.218(18)−3.271(18) Å) and two THF molecules ($Na\cdots O_{THF}$: 2.075(12)/2.345(18) Å), with $Na\cdots O$ distances similar to those previously reported.[73−75]

In the crystal structure of **4** (Figures 2c, S25, and S30), two K^+ ions were bound to the triply reduced $\mathbf{1}^{3-\bullet}$ core forming a monoanionic $[\{K^+(18\text{-crown-}6)(THF)\}_2(\mathbf{1}^{3-})]^-$, which was isolated from the $[K^+(18\text{-crown-}6)(THF)_2]$ moiety. Two K^+ ions (K2 and K2′) were bound to the edge of opposite [4]helicene subunits in η^2-fashions (Figure 2d), and weak cation··· π interactions were observed with relatively long K···C distances (3.514(2)−3.568(2) Å). The coordination of K2 was completed by an equatorial bound 18-crown-6 ether molecule ($K\cdots O_{crown}$: 2.753(2)−2.851(2) Å) and a capping THF molecule ($K\cdots O_{THF}$: 2.690(2) Å), while the K1 ion was solvent-separated by the addition of one more THF molecule ($K\cdots O_{crown}$: 2.749(2)−2.883(2) Å, $K\cdots O_{THF}$: 2.742(7) Å). Notably, $\mathbf{1}^{3-\bullet}$ represents the first example of triply reduced macrocycles, which exhibits a monoradical character with S = 1/2 according to the EPR study (Figure S37).

In contrast, two K^+ ions (K2) in the crystal structure of **5** were η^3-coordinated to the backbone of two opposite [4]helicene subunits (Figures 2e,f, S26, and S31), with the K···C distances ranging over 3.004(4)−3.374(4) Å. Compared to **4**, the K···C distances in **5** were much shorter, and the K2 ion was only hexacoordinated to an 18-crown-6 ether ($K\cdots O_{crown}$: 2.652(9)−3.052(8) Å). The remaining K^+ ions (K1 and K3) were wrapped by an 18-crown-6 ether and two THF molecules, with the $K\cdots O_{crown}$ and $K\cdots O_{THF}$ distances of 2.706(4)−2.855(4) and 2.723(19)/2.735(5) Å, respectively.

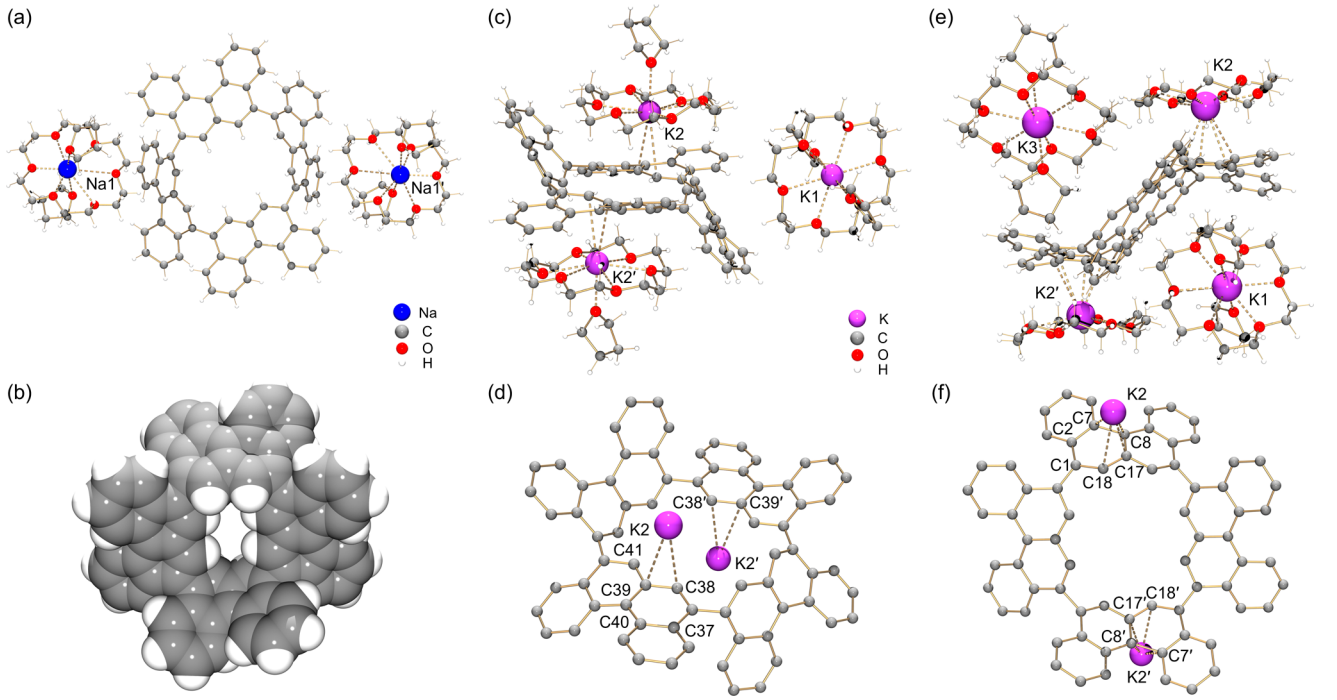

Figure 2. Crystal structure of (a,b) **3** in ball-and-stick model and its $\mathbf{1}^{2-}$ core in space-filling model, crystal structures of (c) **4** and (e) **5**, and metal coordination of (d) **4** and (f) **5** in ball-and-stick models.[24]

https://doi.org/10.1021/prechem.4c00064
Precis. Chem. 2025, 3, 27−34

All of the K···C and K···O distances were close to those reported in the literature.[58,60,76]

Remarkably, the chemical reduction of **1** gives rise to essential structural changes, which can be considered as two major steps and illustrated by the comparison of selected dihedral angles between neutral **1** and its anionic species (Tables 1 and S3−4):

Table 1. Selected Dihedral Angle (deg) of the BH Fragments in 1-n and 3−5

position	1-n	1^{2-} (3)	$1^{3-\bullet}$ (4)	1^{4-} (5)
BH1	81.8	58.7	61.2	38.9
BH2	−65.5	67.7	67.4	83.3
BH3	65.5	−58.7	−61.2	−38.9
BH4	−81.8	−67.7	−67.4	−83.3

(1) From **1** to $\mathbf{1}^{2-}$, the first two-electron addition leads to a *R*/*S* stereo transformation. **1-n** adopts an (*S*,*R*,*S*,*R*)-configuration with the dihedral angles of 81.8°, −65.5°, 65.5°, and −81.8° for its four BH fragments (Figure 1b). Conversely, $\mathbf{1}^{2-}$ presents a less twisted π-framework as reflected by the smaller dihedral angles of 58.7°, 67.7°, −58.7°, and −67.7°, where the inversed value of the dihedral angle for the BH2 and BH3 fragments indicates an *R*/*S* rotation upon two-electron uptake affording an (*S*,*S*,*R*,*R*)-configuration (Figures 2b and S32). Notably, this (*S*,*S*,*R*,*R*)-configuration was allowed to return to the (*S*,*R*,*S*,*R*)-configuration upon oxidation, as confirmed by powder XRD patterns (Figure S33 and Table S5).

(2) From $\mathbf{1}^{2-}$ to $\mathbf{1}^{4-}$, the acceptance of one and two more electrons results in the structural deformation of the π-framework without changing the (*S*,*R*,*S*,*R*)-configuration.

For example, compared to those of $\mathbf{1}^{2-}$, the geometry of $\mathbf{1}^{3-\bullet}$ does not change significantly in view of the dihedral angle for BH fragments (avg 64.3°). In contrast, a noticeable distortion of the π-framework is observed in $\mathbf{1}^{4-}$, as found from the large distinction between the BH1/BH3 (38.9°, −38.9°) and BH2/BH4 fragments (83.3°, −83.3°) according to the dihedral angle, which might stem from direct metal binding of K^+ ions (Figure 2e).

The aromaticity of **1** during chemical reduction was evaluated by density functional theory (DFT) calculations. In neutral **1**, local aromatic currents are observed (Figures 3 and S38). From **1** to $\mathbf{1}^{2-}$, the addition of the first two electrons leads to a reduced aromatic character, which is particularly concentrated at the center of the macrocycle as revealed by IMS3D (Figure 3) and NICS results (Figure S45). From $\mathbf{1}^{2-}$ to $\mathbf{1}^{4-}$, the charged species remain less aromatic in comparison to the neutral parent without noticeable changes. The charges in the anions are always delocalized on the whole π-surface and slightly more dense on the terminal rings (Figure S41).

To understand how stereo transformation of **1** emerged upon the two-electron addition, the NEB-TS calculations were performed using the ORCA program.[77] Given that the (*S*,*R*,*S*,*R*)-to-(*S*,*S*,*R*,*R*) configuration change involves *R*/*S*

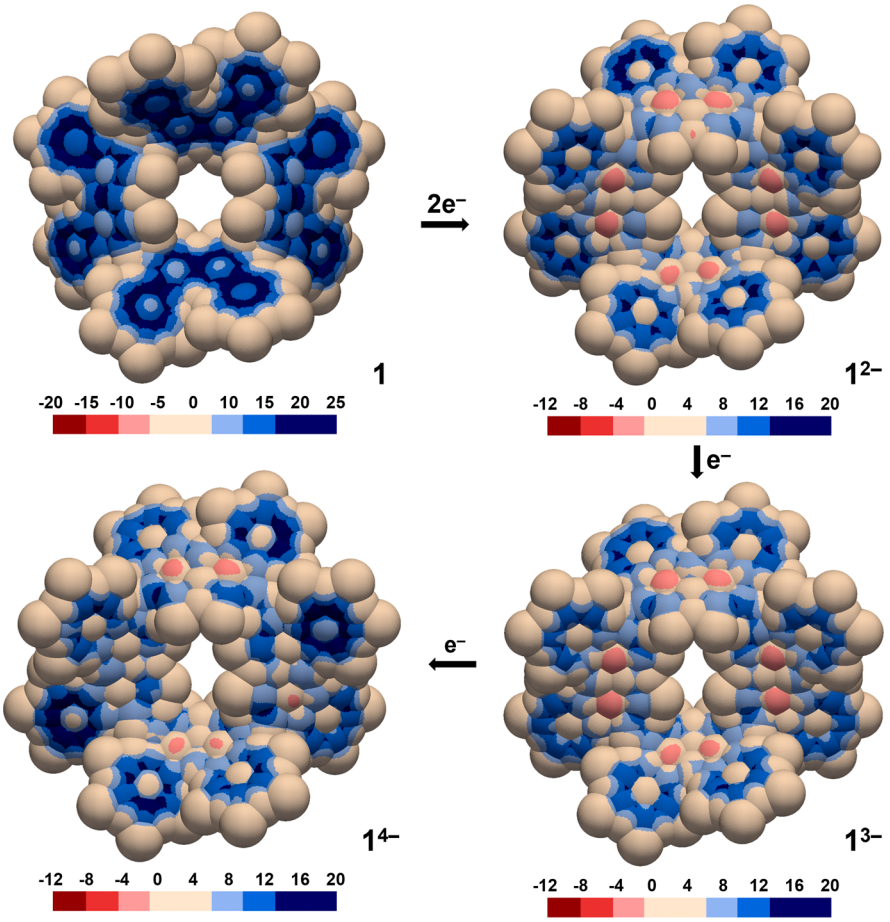

Figure 3. IMS3D maps for (*S*,*R*,*S*,*R*)-**1**, (*S*,*S*,*R*,*R*)-$\mathbf{1}^{2-}$, (*S*,*S*,*R*,*R*)-$\mathbf{1}^{3-\bullet}$, and (*S*,*S*,*R*,*R*)-$\mathbf{1}^{4-}$.

https://doi.org/10.1021/prechem.4c00064
Precis. Chem. 2025, 3, 27−34

rotation of two neighboring BH fragments, we proposed a two-step transformation path to ascertain when the configurational transformation occurs, namely from (*S*,*R*,*S*,*R*)- to (*S*,*R*,*R*,*R*)-, then to (*S*,*S*,*R*,*R*)-**1** at different charging states (neutral, monoanion, and dianion). In all three paths, the (*S*,*R*,*S*,*R*)-conformer remains the most stable (Figure 4 and Table S10).

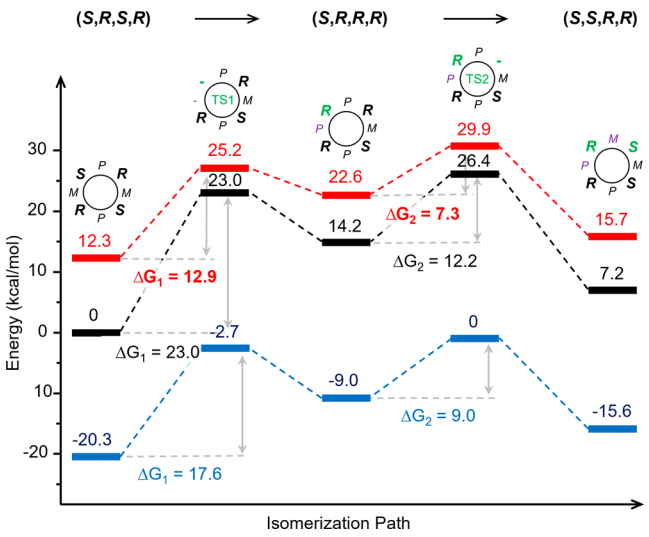

Figure 4. Comparison of the (*S*,*R*,*S*,*R*)-to-(*S*,*S*,*R*,*R*) stereo transformation processes starting from (*S*,*R*,*S*,*R*)-**1** in its neutral (black), monoanionic (blue), and dianionic (red) forms, respectively, with schematic illustrations of the structures of the intermediates and transition states.

Notably, the energy gap of 7.2 kcal/mol between (*S*,*R*,*S*,*R*)- and (*S*,*S*,*R*,*R*)-conformer diminishes as **1** is reduced to monoanion (4.7 kcal/mol) and dianion (3.4 kcal/mol). This trend can also be applied to the energy barriers of TS1 and TS2. For instance, the energy barrier for TS1 in **1** is relatively high (23.0 kcal/mol). Upon reduction of (*S*,*R*,*S*,*R*)-**1** to its monoanion and dianion, a reduced energy requirement for the *S*-to-*R* rotation is evident, as demonstrated by much lower energy barriers of 17.6 and 12.9 kcal/mol, respectively. Similarly, the transformation from the (*S*,*R*,*R*,*R*)- to (*S*,*S*,*R*,*R*)-configuration becomes more approachable in the dianion with an energy barrier of only 7.3 kcal/mol. Such relatively small energy barriers in the dianionic form indicate that the transformation becomes even feasible at room temperature in this charging state.[78] Therefore, we speculate that the stereo transformation of **1** is more favorable upon its two-electron addition due to the largely reduced energy barriers for both isomerization steps (Figures S46–51).

In summary, we synthesized two strained congeners, [4]CH (**1**) and [5]CH (**2**), through one-pot macrocyclization. The structurally rigid BH fragments gave rise to separable *R*/*S*-[*n*]CH stereoisomers. In contrast to **2** where thermal isomerization is applicable for *R*/*S* rotation, the (*S*,*R*,*S*,*R*)-configuration of **1** is thermostable. We therefore explored the stereo transformation process of **1** by charging it with electrons. The chemical reduction of **1** provided ready access to its doubly, triply, and quadruply reduced species, which were all crystallized and characterized by single-crystal X-ray diffraction. The addition of two electrons to **1** enables a reversible transformation of the π-framework between the (*S*,*R*,*S*,*R*)- and (*S*,*S*,*R*,*R*)-configuration, as rationalized by theoretical calculations. More importantly, the (*S*,*S*,*R*,*R*)-configuration of $\mathbf{1}^{2-}$ retains even in its higher charged states ($\mathbf{1}^{3-\bullet}$ and $\mathbf{1}^{4-}$), although the π-framework of $\mathbf{1}^{4-}$ undergoes some structural deformation due to high negative charge and metal coordination. This study not only highlights the power of chemical reduction in affording unstable or inaccessible conformers of polycyclic aromatics but also demonstrates that chemical reduction can effectively modulate the chirality of the hydrocarbon host, suggesting potential applications in chiral molecule separation. Furthermore, the redox-triggered isomerization provides a foundation for designing functional molecular complexes, such as redox-active chiral switches, with the ability to modulate the reactivity and optical or magnetic properties. We are looking forward to uncovering more exciting discoveries from chemical reduction when applied to other π-aromatic systems, as well as their promising applications.

■ ASSOCIATED CONTENT

Supporting Information

The Supporting Information is available free of charge at https://pubs.acs.org/doi/10.1021/prechem.4c00064.

Synthesis details, spectroscopic characterizations, single-crystal X-ray crystallography, and theoretical calculation (PDF)

X-ray crystallographic data (CIF)

Accession Codes

CCDC 2306986–2306993 contain the supplementary crystallographic data for this paper.

■ AUTHOR INFORMATION

Corresponding Authors

Zheng Zhou − *School of Materials Science and Engineering, Tongji University, Shanghai 201804, China;* orcid.org/0000-0001-8905-9663; Email: zhouzheng@tongji.edu.cn

Yong Yang − *School of Chemistry and Chemical Engineering, Southeast University, Nanjing, Jiangsu 211189, China;* Email: yonyan@seu.edu.cn

Authors

Jianwei Liang − *School of Materials Science and Engineering, Tongji University, Shanghai 201804, China;* orcid.org/0000-0003-1849-0864

Sota Sato − *Department of Applied Chemistry, The University of Tokyo, Kashiwa, Chiba 277-0882, Japan; Institute for Molecular Science, Okazaki, Aichi 444-8787, Japan;* orcid.org/0000-0002-7395-2112

Zhenyi Zhang − *Bruker (Beijing) Scientific Technology Co. Ltd., Shanghai 200233, China*

Zheng Wei − *Department of Chemistry, University at Albany, State University of New York, Albany, New York 12222, United States;* orcid.org/0000-0003-4782-021X

Complete contact information is available at: https://pubs.acs.org/10.1021/prechem.4c00064

Notes

The authors declare no competing financial interest.

■ ACKNOWLEDGMENTS

This work received financial support from the National Natural Science Foundation of China (22301219, 22201035), the

Fundamental Research Funds for the Central Universities (22120240039, 2242023R40024), the Start-up Research Fund of Southeast University (RF1028623055), the Shanghai Synchrotron Radiation Facility (2024-NFPS-PT-501026), and JSPS KAKENHI (19H02552). We are grateful to Prof. Hiroyuki Isobe (University of Tokyo) for helpful discussions, and to KEK Photon Factory BL-17A beamline (2023G604 and 2021G589) and SPring-8 BL38B1 and BL45XU beamlines (2018B1394 and 2021B1517) for the access to the X-ray diffraction instruments. We also thank Prof. Yannick Carissan (Aix Marseille Université) for his scientific advice about the IMS3D calculations.

REFERENCES

(1) Iyoda, M.; Yamakawa, J.; Rahman, M. J. Conjugated macrocycles: Concepts and applications. *Angew. Chem., Int. Ed.* **2011**, *50*, 10522−10553.
(2) Segawa, Y.; Yagi, A.; Matsui, K.; Itami, K. Design and synthesis of carbon nanotube segments. *Angew. Chem., Int. Ed.* **2016**, *55*, 5136−5158.
(3) Sun, Z.; Li, K. Recent advances in dimeric cycloparaphenylenes as nanotube fragments. *Synlett* **2021**, *32*, 1581−1587.
(4) Li, Y.; Kono, H.; Maekawa, T.; Segawa, Y.; Yagi, A.; Itami, K. Chemical synthesis of carbon nanorings and nanobelts. *Acc. Mater. Res.* **2021**, *2*, 681−691.
(5) Lewis, S. E. Cycloparaphenylenes and related nanohoops. *Chem. Soc. Rev.* **2015**, *44*, 2221−2304.
(6) Darzi, E. R.; Jasti, R. The dynamic, size-dependent properties of [5]-[12]cycloparaphenylenes. *Chem. Soc. Rev.* **2015**, *44*, 6401−6410.
(7) Toyota, S.; Tsurumaki, E. Exploration of nano-Saturns: A spectacular sphere-ring supramolecular system. *Chem.—Eur. J.* **2019**, *25*, 6878−6890.
(8) Xu, Y.; von Delius, M. The supramolecular chemistry of strained carbon nanohoops. *Angew. Chem., Int. Ed.* **2020**, *59*, 559−573.
(9) Kwon, H.; Bruns, C. J. All-hydrocarbon, all-conjugated cycloparaphenylene-polycyclic aromatic hydrocarbon host-guest complexes stabilized by CH-π interactions. *Nano Res.* **2022**, *15*, 5545−5555.
(10) Matsuno, T.; Isobe, H. Trapped yet free inside the tube: Supramolecular chemistry of molecular peapods. *Bull. Chem. Soc. Jpn.* **2023**, *96*, 406−419.
(11) Xu, Y.; Steudel, F.; Leung, M.-Y.; Xia, B.; von Delius, M.; Yam, V. W. W. [*n*]Cycloparaphenylene-pillar[5]arene bismacrocycles: Their circularly polarized luminescence and multiple guest recognition properties. *Angew. Chem., Int. Ed.* **2023**, *62*, No. e202302978.
(12) Xue, J. Y.; Izumi, T.; Yoshii, A.; Ikemoto, K.; Koretsune, T.; Akashi, R.; Arita, R.; Taka, H.; Kita, H.; Sato, S.; Isobe, H. Aromatic hydrocarbon macrocycles for highly efficient organic light-emitting devices with single-layer architectures. *Chem. Sci.* **2016**, *7*, 896−904.
(13) Leonhardt, E. J.; Jasti, R. Emerging applications of carbon nanohoops. *Nat. Rev. Chem.* **2019**, *3*, 672−686.
(14) Wang, J.; Zhang, X.; Jia, H.; Wang, S.; Du, P. Large π-extended and curved carbon nanorings as carbon nanotube segments. *Acc. Chem. Res.* **2021**, *54*, 4178−4190.
(15) Rapson, W. S.; Shuttleworth, R. G.; van Niekerk, J. N. 89. Benzcyclooctatetraenes. Part III. diphenylene and tetraphenylene. *J. Chem. Soc.* **1943**, 326−327.
(16) Wittig, G.; Rümpler, K.-D. Über die reaktionsweise von 2.2′-dilithium-biphenyl gegenüber metallhalogeniden, III. die atropisomeren *o*-hexaphenylene. *Justus Liebigs Ann. Chem.* **1971**, *751*, 1−16.
(17) Irngartinger, H. The crystal and molecular structures of the centrosymmetric hexa-*o*-phenylene. *Isr. J. Chem.* **1972**, *10*, 635−647.
(18) Staab, H. A.; Binnig, F. Synthese und eigenschaften von hexa-*m*-phenylen. *Tetrahedron Lett.* **1964**, *5*, 319−321.
(19) Staab, H. A.; Binnig, F. Zur konjugation in makrocyclischen bindungssystemen, VII. Synthese und eigenschaften von hexa-*m*-phenylen und octa-*m*-phenylen. *Chem. Ber.* **1967**, *100*, 293−305.
(20) Jasti, R.; Bhattacharjee, J.; Neaton, J. B.; Bertozzi, C. R. Synthesis, characterization, and theory of [9]-, [12]-, and [18]-cycloparaphenylene: Carbon nanohoop structures. *J. Am. Chem. Soc.* **2008**, *130*, 17646−17647.
(21) Majewski, M. A.; Stepien, M. Bowls, hoops, and saddles: Synthetic approaches to curved aromatic molecules. *Angew. Chem., Int. Ed.* **2019**, *58*, 86−116.
(22) Mirzaei, S.; Castro, E.; Hernandez Sánchez, R. Conjugated molecular nanotubes. *Chem.—Eur. J.* **2021**, *27*, 8642−8655.
(23) Hermann, M.; Wassy, D.; Esser, B. Conjugated nanohoops incorporating donor, acceptor, hetero- or polycyclic aromatics. *Angew. Chem., Int. Ed.* **2021**, *60*, 15743−15766.
(24) Lorbach, D.; Keerthi, A.; Figueira-Duarte, T. M.; Baumgarten, M.; Wagner, M.; Müllen, K. Cyclization of pyrene oligomers: Cyclohexa-1,3-pyrenylene. *Angew. Chem., Int. Ed.* **2016**, *55*, 418−421.
(25) Kurosaki, R.; Suzuki, M.; Hayashi, H.; Fujiki, M.; Aratani, N.; Yamada, H. Torsional chirality generation based on cyclic oligomers constructed from an odd number of pyrenes. *Chem. Commun.* **2019**, *55*, 9618−9621.
(26) Okada, K.; Yagi, A.; Segawa, Y.; Itami, K. Synthesis and properties of [8]-, [10]-, [12]-, and [16]cyclo-1,4-naphthylenes. *Chem. Sci.* **2017**, *8*, 661−667.
(27) Yang, Y.; Nanjo, Y.; Isobe, H.; Sato, S. Synthesis and stereoisomerism of [*n*]cyclo-2,9-phenanthrenylene congeners possessing alternating *E*/*Z*- and *R*/*S*-biaryl linkages. *Org. Biomol. Chem.* **2020**, *18*, 4949−4955.
(28) Kurosaki, R.; Morimoto, H.; Matsuo, K.; Hayashi, H.; Yamada, H.; Aratani, N. An atropisomerism study of large cycloarylenes: [*n*]Cyclo-4,10-pyrenylenes' case. *Chem.-Eur. J.* **2023**, *29*, No. e202203848.
(29) Robert, A.; Naulet, G.; Bock, H.; Vanthuyne, N.; Jean, M.; Giorgi, M.; Carissan, Y.; Aroulanda, C.; Scalabre, A.; Pouget, E.; Durola, F.; Coquerel, Y. Cyclobishelicenes: Shape-persistent figure-eight aromatic molecules with promising chiroptical properties. *Chem.-Eur. J.* **2019**, *25*, 14364−14369.
(30) Nakanishi, W.; Matsuno, T.; Ichikawa, J.; Isobe, H. Illusory molecular expression of "Penrose Stairs" by an aromatic hydrocarbon. *Angew. Chem., Int. Ed.* **2011**, *50*, 6048−6051.
(31) Robert, A.; Dechambenoit, P.; Hillard, E. A.; Bock, H.; Durola, F. Non-planar oligoarylene macrocycles from biphenyl. *Chem. Commun.* **2017**, *53*, 11540−11543.
(32) Naulet, G.; Sturm, L.; Robert, A.; Dechambenoit, P.; Röhricht, F.; Herges, R.; Bock, H.; Durola, F. Cyclic tris-[5]helicenes with single and triple twisted Möbius topologies and Möbius aromaticity. *Chem. Sci.* **2018**, *9*, 8930−8936.
(33) Malinčík, J.; Gaikwad, S.; Mora-Fuentes, J. P.; Boillat, M.-A.; Prescimone, A.; Häussinger, D.; Campaña, A. G.; Šolomek, T. Circularly polarized luminescence in a Möbius helicene carbon nanohoop. *Angew. Chem., Int. Ed.* **2022**, *61*, No. e202208591.
(34) Aribot, F.; Merle, A.; Dechambenoit, P.; Bock, H.; Artigas, A.; Vanthuyne, N.; Carissan, Y.; Hagebaum-Reignier, D.; Coquerel, Y.; Durola, F. A triply [5]helicene-bridged (1,3,5)cyclophane. *Angew. Chem., Int. Ed.* **2023**, *62*, No. e202304058.
(35) Hitosugi, S.; Nakanishi, W.; Isobe, H. Atropisomerism in a belt-persistent nanohoop molecule: Rotational restriction forced by macrocyclic ring strain. *Chem.-Asian J.* **2012**, *7*, 1550−1552.
(36) Sarkar, P.; Sun, Z.; Tokuhira, T.; Kotani, M.; Sato, S.; Isobe, H. Stereoisomerism in nanohoops with heterogeneous biaryl linkages of *E*/*Z*- and *R*/*S*-geometries. *ACS Cent. Sci.* **2016**, *2*, 740−747.
(37) Sun, Z.; Suenaga, T.; Sarkar, P.; Sato, S.; Kotani, M.; Isobe, H. Stereoisomerism, crystal structures, and dynamics of belt-shaped cyclonaphthylenes. *Proc. Natl. Acad. Sci. U. S. A.* **2016**, *113*, 8109−8114.
(38) Sun, Z.; Matsuno, T.; Isobe, H. Stereoisomerism and structures of rigid cylindrical cycloarylenes. *Bull. Chem. Soc. Jpn.* **2018**, *91*, 907−921.
(39) Wang, J.; Zhuang, G.; Chen, M.; Lu, D.; Li, Z.; Huang, Q.; Jia, H.; Cui, S.; Shao, X.; Yang, S.; Du, P. Selective synthesis of conjugated chiral macrocycles: Sidewall segments of (−)/(+)-(12,4) carbon

nanotubes with strong circularly polarized luminescence. *Angew. Chem., Int. Ed.* **2020**, *59*, 1619−1626.
(40) Hasegawa, M.; Nojima, Y.; Mazaki, Y. Circularly polarized luminescence in chiral π-conjugated macrocycles. *ChemPhotoChem.* **2021**, *5*, 1042−1058.
(41) Wang, J.-Q.; Han, X.-N.; Han, Y.; Chen, C.-F. Advances in circularly polarized luminescence materials based on chiral macrocycles. *Chem. Commun.* **2023**, *59*, 13089−13106.
(42) Hasegawa, M.; Mazaki, Y. Stereogenic π-conjugated macrocycles: Synthesis, structure, and chiroptical properties including circularly polarized luminescence. *Synlett* **2023**, *35*, 1361−1374.
(43) Rickhaus, M.; Mayor, M.; Juríček, M. Chirality in curved polyaromatic systems. *Chem. Soc. Rev.* **2017**, *46*, 1643−1660.
(44) Fujitsuka, M.; Tojo, S.; Iwamoto, T.; Kayahara, E.; Yamago, S.; Majima, T. Radical ions of cyclopyrenylene: Comparison of spectral properties with cycloparaphenylene. *J. Phys. Chem. A* **2015**, *119*, 4136−4141.
(45) Kayahara, E.; Kouyama, T.; Kato, T.; Yamago, S. Synthesis and characterization of [*n*]CPP (*n* = 5, 6, 8, 10, and 12) radical cation and dications: Size-dependent absorption, spin, and charge delocalization. *J. Am. Chem. Soc.* **2016**, *138*, 338−344.
(46) Ozaki, N.; Sakamoto, H.; Nishihara, T.; Fujimori, T.; Hijikata, Y.; Kimura, R.; Irle, S.; Itami, K. Electrically activated conductivity and white light emission of a hydrocarbon nanoring-iodine assembly. *Angew. Chem., Int. Ed.* **2017**, *56*, 11196−11202.
(47) Wu, D.; Cheng, W.; Ban, X.; Xia, J. Cycloparaphenylenes (CPPs): An overview of synthesis, properties, and potential applications. *Asian J. Org. Chem.* **2018**, *7*, 2161−2181.
(48) Masumoto, Y.; Toriumi, N.; Muranaka, A.; Kayahara, E.; Yamago, S.; Uchiyama, M. Near-infrared fluorescence from In-plane-aromatic cycloparaphenylene dications. *J. Phys. Chem. A* **2018**, *122*, 5162−5167.
(49) Alvarez, M. P.; Ruiz Delgado, M. C.; Taravillo, M.; Baonza, V. G.; Lopez Navarrete, J. T.; Evans, P.; Jasti, R.; Yamago, S.; Kertesz, M.; Casado, J. The Raman fingerprint of cyclic conjugation: the Case of the stabilization of cations and dications in cycloparaphenylenes. *Chem. Sci.* **2016**, *7*, 3494−3499.
(50) Zabula, A. V.; Spisak, S. N.; Filatov, A. S.; Rogachev, A. Yu.; Petrukhina, M. A. Record alkali metal intercalation by highly charged corannulene. *Acc. Chem. Res.* **2018**, *51*, 1541−1549.
(51) Zhou, Z.; Petrukhina, M. A. Planar, curved and twisted molecular nanographenes: Reduction-induced alkali metal coordination. *Coord. Chem. Rev.* **2023**, *486*, 215144.
(52) Wombacher, T.; Goddard, R.; Lehmann, C. W.; Schneider, J. J. Complete charge separation provoked by full cation encapsulation in the radical mono- and di-anions of 5,6:11,12-di-*o*-phenylenetetracene. *Dalton Trans.* **2018**, *47*, 10874−10883.
(53) Li, B.; Yang, C.; Wang, X.; Li, G.; Peng, W.; Xiao, H.; Luo, S.; Xie, S.; Wu, J.; Zeng, Z. Synthesis and structural elucidation of bisdibenzocorannulene at redox states. *Angew. Chem., Int. Ed.* **2021**, *60*, 19790−19796.
(54) Wang, W.; Ma, X.-H.; Liu, M.; Tang, S.; Ding, X.; Zhao, Y.; Tan, Y.; Kertesz, M.; Wang, X. A triply negatively charged nanographene bilayer with spin frustration. *Angew. Chem., Int. Ed.* **2023**, *62*, No. e202217788.
(55) Stawski, W.; Zhu, Y.; Rončević, I.; Wei, Z.; Petrukhina, M. A.; Anderson, H. L. The anti-aromatic dianion and aromatic tetraanion of [18]annulene. *Nat. Chem.* **2024**, *16*, 998−1002.
(56) Spisak, S. N.; Wei, Z.; Darzi, E.; Jasti, R.; Petrukhina, M. A. Highly strained [6]cycloparaphenylene: Crystallization of an unsolvated polymorph and the first mono- and dianions. *Chem. Commun.* **2018**, *54*, 7818−7821.
(57) Zhou, Z.; Wei, Z.; Schaub, T. A.; Jasti, R.; Petrukhina, M. A. Structural deformation and host-guest properties of doubly-reduced cycloparaphenylenes, [*n*]CPPs^{2-} (*n* = 6, 8, 10, and 12). *Chem. Sci.* **2020**, *11*, 9395−9401.
(58) Zabula, A. V.; Filatov, A. S.; Xia, J.; Jasti, R.; Petrukhina, M. A. Tightening of the nanobelt upon multielectron reduction. *Angew. Chem., Int. Ed.* **2013**, *52*, 5033−5036.
(59) Rogachev, A. Yu.; Zhou, Z.; Liu, S.; Wei, Z.; Schaub, T. A.; Jasti, R.; Petrukhina, M. A. Stretching [8]cycloparaphenylene with encapsulated potassium cations: Structural and theoretical insights into core perturbation upon four-fold reduction and complexation. *Chem. Sci.* **2021**, *12*, 6526−6535.
(60) Zhou, Z.; Wei, Z.; Ikemoto, K.; Sato, S.; Isobe, H.; Petrukhina, M. A. Chemical reduction of nanosized [6]cyclo-2,7-naphthylene macrocycle. *Angew. Chem., Int. Ed.* **2021**, *60*, 11201−11205.
(61) Spisak, S. N.; Zabula, A. V.; Alkan, M.; Filatov, A. S.; Rogachev, A. Yu.; Petrukhina, M. A. Site-directed dimerization of bowl-shaped radical anions to form a σ-bonded dibenzocorannulene dimer. *Angew. Chem., Int. Ed.* **2018**, *57*, 6171−6175.
(62) Zhou, Z.; Zhu, Y.; Wei, Z.; Bergner, J.; Neiß, C.; Doloczki, S.; Görling, A.; Kivala, M.; Petrukhina, M. A. Reduction of π-expanded cyclooctatetraene with lithium: Stabilization of the tetraanion through internal Li^+ coordination. *Angew. Chem., Int. Ed.* **2021**, *60*, 3510−3514.
(63) Zhou, Z.; Zhu, Y.; Wei, Z.; Bergner, J.; Neiß, C.; Doloczki, S.; Görling, A.; Kivala, M.; Petrukhina, M. A. Reversible structural rearrangement of π-expanded cyclooctatetraene upon two-fold reduction with alkali metals. *Chem. Commun.* **2022**, *58*, 3206−3209.
(64) Pennachio, M.; Wei, Z.; Clevenger, R. G.; Kilway, K. V.; Tsybizova, A.; Gershoni-Poranne, R.; Petrukhina, M. A. Repercussions of multi-electron uptake by a twistacene: a reduction-induced double dehydrogenative annulation. *Org. Chem. Front.* **2023**, *10*, 5823−5833.
(65) Zhou, Z.; Kawade, R. K.; Wei, Z.; Kuriakose, F.; Üngör, Ö.; Jo, M.; Shatruk, M.; Gershoni-Poranne, R.; Petrukhina, M. A.; Alabugin, I. V. Negative charge as a lens for concentrating antiaromaticity: Using a pentagonal "defect" and helicene strain for cyclizations. *Angew. Chem., Int. Ed.* **2020**, *59*, 1256−1262.
(66) Zhou, Z.; Egger, D. T.; Hu, C.; Pennachio, M.; Wei, Z.; Kawade, R. K.; Üngör, Ö.; Gershoni-Poranne, R.; Petrukhina, M. A.; Alabugin, I. V. Localized antiaromaticity hotspot drives reductive dehydrogenative cyclizations in bis- and mono-helicenes. *J. Am. Chem. Soc.* **2022**, *144*, 12321−12338.
(67) Zhou, Z.; Pennachio, M.; Wei, Z.; Heldner, M. L.; Petrukhina, M. A.; Schaub, T. A. Synthesis, structural characterization, and reductive cleavage of an oxygen-containing naphthyl macrocycle. *Eur. J. Org. Chem.* **2023**, *26*, No. e202300168.
(68) Xue, J. Y.; Ikemoto, K.; Takahashi, N.; Izumi, T.; Taka, H.; Kita, H.; Sato, S.; Isobe, H. Cyclo-*meta*-phenylene revisited: Nickel-mediated synthesis, molecular structures, and device applications. *J. Org. Chem.* **2014**, *79*, 9735−9739.
(69) Yamamoto, Y.; Tsurumaki, E.; Wakamatsu, K.; Toyota, S. Nano-saturn: Experimental evidence of complex formation of an anthracene cyclic ring with C_{60}. *Angew. Chem., Int. Ed.* **2018**, *57*, 8199−8202.
(70) Tian, Y.; Ikemoto, K.; Sato, S.; Isobe, H. [*n*]Cyclo-3,6-phenanthrenylenes: Synthesis, structure, and fluorescence. *Chem.-Asian J.* **2017**, *12*, 2093−2097.
(71) Ikemoto, K.; Sato, S.; Isobe, H. One-pot synthesis of [*n*]cyclo-1,3-pyrenylenes via Ni-mediated macrocyclization. *Chem. Lett.* **2016**, *45*, 217−219.
(72) Miyahara, T.; Shimizu, M. Single crystal growth of organic semiconductors by the repeated solid solvent growth method using melted anthracene as a solvent. *J. Cryst. Growth* **2001**, *229*, 553−557.
(73) Zhou, Z.; Wei, Z.; Tokimaru, Y.; Ito, S.; Nozaki, K.; Petrukhina, M. A. Stepwise reduction of azapentabenzocorannulene. *Angew. Chem., Int. Ed.* **2019**, *58*, 12107−12111.
(74) Zhang, Y.; Zhu, Y.; Lan, D.; Pun, S. H.; Zhou, Z.; Wei, Z.; Wang, Y.; Lee, H. K.; Lin, C.; Wang, J.; Petrukhina, M. A.; Li, Q.; Miao, Q. Charging a negatively curved nanographene and its covalent network. *J. Am. Chem. Soc.* **2021**, *143*, 5231−5238.
(75) Zhou, Z.; Zhu, Y.; Fernández-García, J. M.; Wei, Z.; Fernández, I.; Petrukhina, M. A.; Martín, N. Stepwise reduction of a corannulene-based helical molecular nanographene with Na metal. *Chem. Commun.* **2022**, *58*, 5574−5577.

https://doi.org/10.1021/prechem.4c00064
Precis. Chem. 2025, 3, 27−34

(76) Guo, Y.; Torchon, H. S.; Zhu, Y.; Wei, Z.; Zhang, Z.; Han, H.; Petrukhina, M. A.; Zhou, Z. Stepwise deprotonation of truxene: Structures, metal complexation and charge-dependent optical properties. *Chem. Sci.* **2023**, *14*, 13219−13227.
(77) Neese, F.; Wennmohs, F.; Becker, U.; Riplinger, C. The ORCA quantum chemistry program package. *J. Chem. Phys.* **2020**, *152*, 224108.
(78) Rickhaus, M.; Mayor, M.; Juríček, M. Strain-induced helical chirality in polyaromatic systems. *Chem. Soc. Rev.* **2016**, *45*, 1542−1556.

https://doi.org/10.1021/prechem.4c00064
Precis. Chem. 2025, 3, 27−34